Materials Research. 2014; 17(Suppl. 1): 133-140
DOI: http://dx.doi.org/10.1590/S1516-14392014005000060
© 2014

Synthesis and Characterization of Water-dispersed CdSe/CdS Core-shell Quantum Dots Prepared via Layer-by-layer Method Capped with Carboxylic-functionalized Poly(Vinyl Alcohol)

Fábio Pereira Ramanery, Alexandra Ancelmo Piscitelli Mansur, Herman Sander Mansur*

Center of Nanoscience, Nanotechnology and Innovation-CeNano²I, Department of Metallurgical and Materials Engineering, Federal University of Minas Gerais – UFMG, Av. Antônio Carlos, 6627, Escola de Engenharia, Bloco 2/2233, Pampulha, CEP 31270-901, Belo Horizonte, MG, Brazil

Received: June 27, 2013; Revised: April 9, 2014

The main goal of this work was to synthesize CdSe/CdS (core-shell) nanoparticles stabilized by polymer ligand using entirely aqueous colloidal chemistry at room temperature. First, the CdSe core was prepared using precursors and acid-functionalized poly(vinyl alcohol) as the capping ligand. Next, a CdS shell was grown onto the CdSe core *via* the layer-by-layer technique. The CdS shell was formed by two consecutive monolayers, as estimated by empirical mathematical functions. The nucleation and growth of CdSe quantum dots followed by CdS shell deposition were characterized by UV-vis spectroscopy, photoluminescent (PL) spectroscopy and transmission electron microscopy (TEM). The results indicated a systematic red-shift of the absorption and emission spectra after the deposition of CdS, indicating the shell growth onto the CdSe core. TEM coupled with electron diffraction analysis revealed the presence of CdSe/CdS with an epitaxial shell growth. Therefore, it may be concluded that CdSe/CdS quantum dots with core-shell nanostructure were effectively synthesized.

Keywords: *nanomaterial, colloid, nanotechnology, semiconductor, polymer*

1. Introduction

Quantum dots (QDs) are nanocrystals (typically 1-10 nm in diameter) of inorganic semiconductor materials (usually groups II-VI or III-V semiconductors). They represent one of the most exciting nano-science fields of the current century, primarily due to the drastic changes in most properties of materials dependent on the nanocrystal size due to quantum confinement[1,2]. Among several semiconductor possibilities, cadmium selenide (CdSe) is one of the most versatile quantum dot materials, as its emission peak can be anywhere in the visible spectrum, with potential applications ranging from solar-light sensitizers to multicolor fluorescent markers in biological systems[3]. The most common preparation route for CdSe nanoparticles involves hot-matrix synthesis in organic solvents. Water-based synthesis has also been developed for the preparation of colloidal CdSe QDs, offering a greener, simpler, faster, and often room-temperature method. However, the organometallic approaches are assumed to produce higher-quality QDs in terms of the overall control of size, shape, and quantum yield of emission[3-5].

The polymer coating of QDs is considered a powerful tool for diagnostics and sensing applications[4], and our research group is focusing on the development of hybrid nanomaterials based on biocompatible polymers, especially by combining organic ligands and inorganic nanoparticles with proteins and carbohydrates, for a myriad of novel applications[6-11]. In these previous studies, poly(vinyl alcohol) (PVA) and its derivatives, such as PVA with carboxylic groups (PVA-COOH), have been our preferred choice for preparing colloidal suspensions due to their water-solubility, biocompatibility, and biodegradability, aiming at medical, biological and pharmaceutical applications[12,13].

In this work, the main goal was the synthesis and characterization of CdSe/CdS core-shell nanostructures with enhanced fluorescent properties using an aqueous colloidal route at room temperature and carboxylated-PVA as the biocompatible capping agent for potential biomarker applications.

2. Material and Methods

2.1. *Chemicals*

All reagents and precursors, metallic selenium powder (PA > 99%), cadmium perchlorate hydrate (Aldrich, Cat#401374, $Cd(ClO_4)_2 \cdot 6H_2O$), sodium sulfite (VETEC, >98%, Na_2SO_3), thioacetamide (Sigma-Aldrich, Cat#163678, CH_3CSNH_2, > 99%), and ammonium hydroxide (PA, Synth, NH_4OH, NH_3: 28-30%), were used as received, without any further purification. Chemically functionalized PVA containing 1.0 mol% carboxylic acid units (PVA-COOH) was donated by Kuraray Corporation (Poval KM-118, M_w = 85,000-124,000 g/mol, degree of hydrolysis = 95.5-98.5%). De-ionized water (DI water, Millipore Simplicity™) with a resistivity of 18 MΩ·cm was used in all solutions.

*e-mail: hmansur@demet.ufmg.br

2.2. *Synthesis of CdSe core nanoparticles in PVA-COOH solutions*

The precursors for the synthesis of quantum dots were prepared according to similar procedures previously reported by our group[6,7].

In brief, CdSe nanoparticles were synthesized *via* an aqueous route in a reaction flask using the previously prepared stock solutions, with Cd^{2+} and Se^{2-} as precursors and PVA-COOH as the capping polymer. The simplified reaction is presented in Equation 1.

$$Cd^{2+}_{(aq)} + SeSO_3^{2-}{}_{(aq)} + 2OH^-_{(aq)} \rightarrow CdSe_{(s,\ colloidal)} + SO_4^{2-}{}_{(aq)} + H_2O_{(l)} \quad (1)$$

A typical synthesis was carried out as follows. First, 2 mL of PVA-COOH solution and 45 mL of DI water were added to the flask reacting vessel (pH = 10.5±0.2 adjusted with NH_4OH). Next, under stirring with a shaker, the cadmium precursor ($Cd(ClO_4)_2 \cdot 6H_2O$) and selenide source solution (Na_2SeSO_3) were added to the flask to obtain a cadmium-to-selenium molar ratio of 2.0:0.75 (Cd:Se-2.0:0.75). The solution was then allowed to sit for 2 h.

2.3. *Synthesis of CdSe/CdS (core-shell) nanoparticles in PVA-COOH solutions*

The shell growth was designed to be performed using a layer-by-layer (LBL) approach, following the so-called successive ion layer adsorption and reaction (SILAR) method. Based on the molar quantity of nanocrystals in the CdSe core colloidal solution and the size of these nanoparticles, the amount of precursor for growing each monolayer of a shell of CdS on the nanoparticle surface was calculated using parameters of the CdS bulk crystal as follows (Equations 2, 3 and 4)[14]:

$$V_{CdS} = \frac{4}{3}\pi\left[\left(R_{AB} + d\right)^3 - R_{AB}^3\right] \quad (2)$$

$$n_{CdS} = \frac{\rho_{CdS} V_{CdS} 10^{-27}}{m_{CdS}} \quad (3)$$

$$M_{CdS} = n_{AB} n_{CdS} \quad (4)$$

where V_{CdS} is the volume of the shell comprising one monolayer (nm^3), R_{AB} is the radius of the nanocrystal to be overgrown (nm) by the shell, d is the thickness of one shell monolayer (nm), n_{CdS} is the number of CdS monomer units per nanocrystal contained in one monolayer (dimensionless), ρ_{CdS} is the density of the bulk shell material ($kg.m^{-3}$), m_{CdS} is the mass of a shell monomer unit (kg), M_{CdS} is the molar quantity of Cd^{2+} and S^{2-} precursors needed to grow one monolayer (mmol), and n_{AB} is the molar quantity of core used for the synthesis of the core-shell system (mmol).

For the CdS shell, ρ_{CdS} was considered to be 4820 $kg.m^{-3}$, and the thickness of one monolayer was 0.35 nm (an approximately 0.7 nm increase in diameter per layer). The definition of a monolayer here is a CdS shell that is approximately 0.35 nm thick, corresponding to the distance between consecutive planes along the axis in bulk wurtzite CdS[10]. Additionally, the term "monomer" represents the hypothetical smallest subunit of the shell material consisting of one Cd^{2+} cation and one S^{2-} anion.

The first "adlayer" of CdS was grown onto Cd:Se at a molar ratio of 2:0.75, producing a core-shell (C-S) nanostructure (CdSe/CdS). In this case, there is an excess of Cd^{2+} in solution from the core preparation stage, and only the calculated amount of sulfide precursor required to produce a CdS monolayer was added to the system under stirring. In the sequence, the second monolayer was created by alternating the injections of cationic and anionic precursors, slowly adding the precursors dropwise to the colloidal media at 23±2 °C and pH = 10.5±0.5, as adjusted using NH_4OH. Figure 1 presents a schematic representation of the synthesis procedure for CdSe/CdS core-shell nanostructures.

2.4. *UV-visible (UV-vis) spectroscopy characterization*

UV-vis spectroscopy measurements were conducted using a Perkin-Elmer (Lambda EZ-210) spectrophotometer in the wavelength range of 700 to 190 nm in transmission mode using a quartz cuvette. The absorption spectra were used to monitor the formation of CdSe and CdSe/CdS nanoparticles and their relative colloidal stabilities in the media. All experiments were conducted in triplicate (n = 3) unless specifically noted. Statistical analysis was performed to obtain the average and standard deviation of the results where applicable.

2.5. *Photoluminescence spectroscopy characterization (PL)*

The emission spectra of the CdSe and CdSe/CdS nanoparticles were acquired using an Ocean Optics USB4000 VIS-NIR spectrophotometer and a helium-cadmium (He:Cd) laser at $\lambda_{excitation}$ = 442 nm (violet-blue, 15 mW of power) as the excitation source. All of the photoluminescence (PL) spectra were collected at room temperature.

To verify the relative fluorescence intensities, the emission spectra of the CdSe nanocrystals and core-shell CdSe/CdS nanoparticles were collected using a Nanodrop 3300 fluoro-spectrometer (Thermo Scientific). The excitation source was a solid-state light-emitting diode (LED) with $\lambda_{excitation}$ = 365±10 nm equipped with a cut-filter that eliminates excitation above 400 nm. All of the photoluminescence (PL) spectra were collected at room temperature, and the measurements of fluorescence intensities were reported in relative fluorescent units (RFU) at the wavelength at which the emission spectra reached the maximum intensity. The relative activity was calculated by subtracting the background of the samples without QDs.

2.6. *Transmission Electron Microscopy (TEM)/ Energy-Dispersive X-Ray Spectroscopy (EDS) characterization*

The QD size and distribution data were assessed using transmission electron microscopy (Tecnai G2–Spirit-FEI) at 200 kV coupled to EDS. These values were obtained by measuring at least 100 individual nanoparticles using an

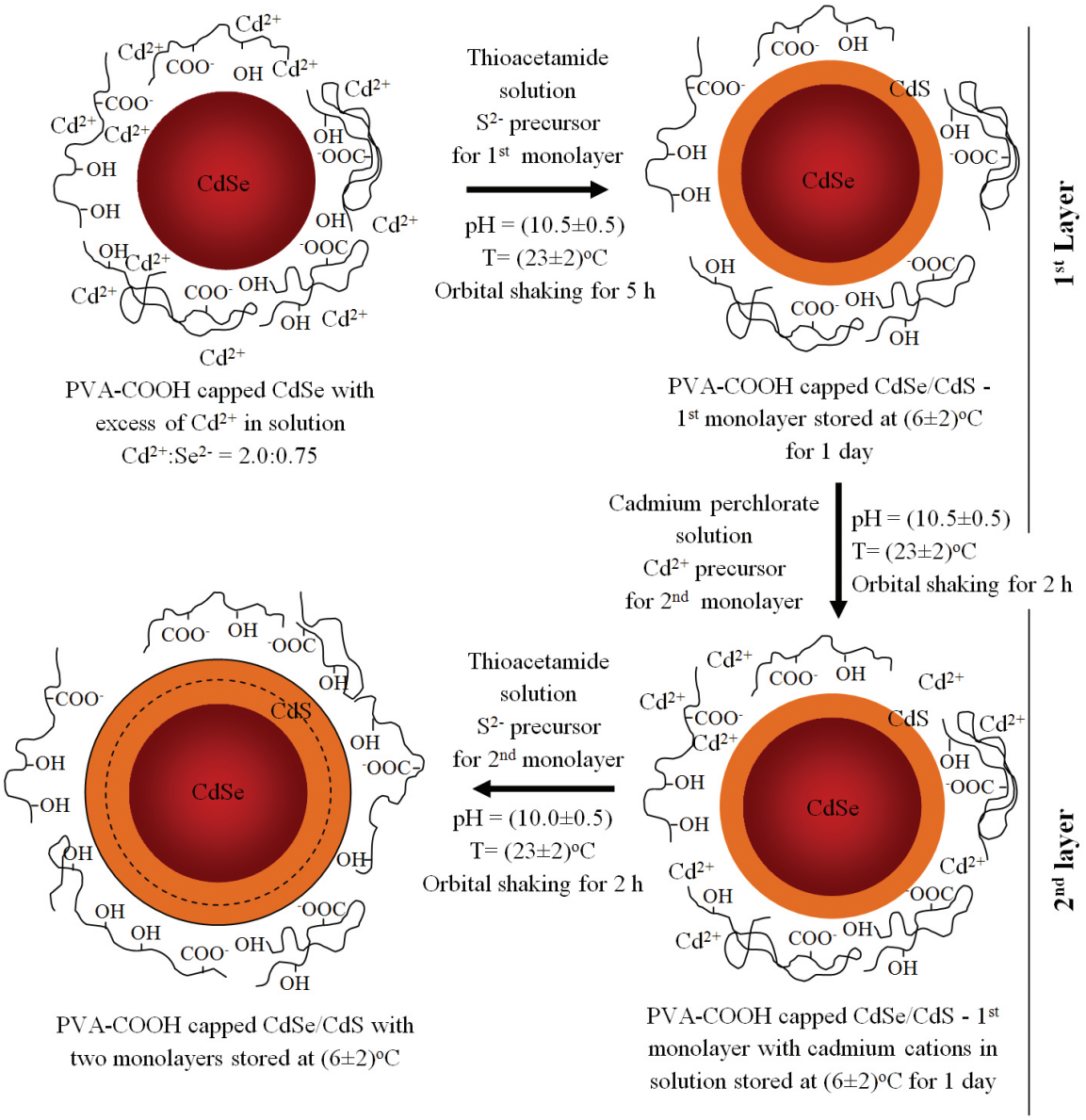

Figure 1. Representation of the designed experimental procedure for the CdS/CdSe-PVA-COOH colloidal system.

image-processing program (ImageJ, version 1.44, public domain, National Institute of Mental Health).

In all TEM analyses, samples were prepared by dropping the colloidal dispersion onto a holey carbon grid after the purification. Briefly, the purification was carried out using an ultracentrifuge (Hettich Mikro 200R) with cut-off cellulose membranes (Amicon filter, Millipore, 60 kDa) to remove excess reagents. Centrifugation was conducted for 30 min (6 cycles × 5 min per cycle, 12,000 rpm). After the first cycle, the sample was washed five times with 400 µL of DI water.

3. Results and Discussion

Figure 2a shows the UV-vis spectra of CdSe quantum dots ("core") after three days of preparation. Because of their ultra-small size, semiconductor nanoparticles with dimensions below the Bohr radius (a_B) will present a quantum-confinement effect related to the strong interaction between the hole-electron pair generated by the exciting photon[1]. The quasi-particle created by this bound state of an electron (e^-) and a hole (h^+) is referred to as an exciton. The position of the excitonic peak ("shoulder"), λ_{exc}, may be observed in the UV-vis absorption spectrum as an abrupt increase in absorbance at 500-650 nm as evidence of CdSe nanoparticle quantum confinement stabilized by the PVA-COOH ligand.

The wavelength value (λ_{QD}) associated with the "absorbance onset" was determined using the optical band gap (E_{QD}) once it has been accepted as a more accurate method for its evaluation. This optical band gap is the lowest

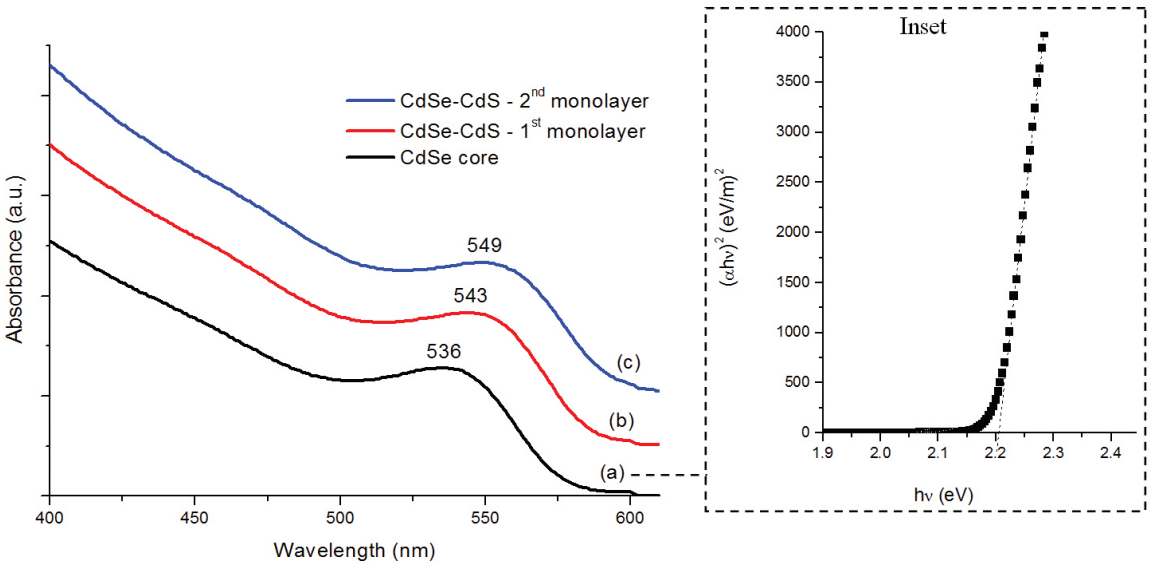

Figure 2. UV–vis spectra of the CdSe core (a), CdSe/CdS – 1st monolayer (b) and CdSe/CdS – 2nd monolayer (c) after three days of preparation. Inset: Optical absorption spectrum of the CdSe core nanoparticles.

excitation energy of the quantum dots and was estimated from absorption coefficient data as a function of wavelength using the "Tauc relation"[7], as shown in Equation 5:

$$\alpha h\nu = B\left(h\nu - E_{QD}\right)^{n} \quad (5)$$

where α is the absorption coefficient, hν is the photon energy, B is the band form parameter, and n = ½ for a direct band gap and 2 for an indirect band gap. In this case, n = ½, as CdSe is a direct-band-gap semiconductor[7]. Therefore, one can estimate the direct band gap value from the plots of $(\alpha h\nu)^2$ versus (hν) and extrapolating the straight portion of the graph to the (hν) axis, i.e., α = 0 (Figure 2, inset).

The average core sizes were determined using the empirical fitting functions (Equation 6) reported by Yu et al.[15] considering the restrictions for its application.

$$2R_{AB} = 1.6122\times10^{-9}\lambda_{exc}^{4} - 2.6575\times10^{-6}\lambda_{exc}^{3} + 1.6242\times10^{-3}\lambda_{exc}^{2} - 4.277\times10^{-1}\lambda_{exc} + 41.57 \quad (6)$$

The size distribution of the nanoparticles was also estimated using the "half-width at half-maximum" (HWHM) extracted from the UV-vis spectroscopy curves (not shown). According to Dai et al.[16], the HWHM on the low-energy side of the first exciton absorption peak can be used as suitable indicator of the size distribution, with smaller HWHM values corresponding to narrower size distributions.

Assuming Beer-Lambert Law behavior, the absorbance of the dispersion containing quantum dots is proportional to the concentration (and number of nuclei) and therefore can be accessed from the UV-vis spectra. However, as the extinction coefficient (ε) is size-dependent, empirical mathematical functions were developed by Yu et al.[15] to calculate ε (Equation 7).

$$\varepsilon = 5857\left(R_{AB}\right)^{2.65} \quad (7)$$

Table 1. Quantum dot parameters.

Parameter	Unit	CdSe core
E_{QD}	(eV)	(2.20±0.05)
λ_{QD}	(nm)	(563±6)
λ_{exc}	(nm)	(541±4)
E_g^{exc}	(eV)	(2.29±0.02)
Abs	-	(0.055±0.010)
HWHM	(nm)	(26±2)
$2R_{AB}$ (average)	(nm)	(2.9±0.1)
ε	$(L.mol^{-1}.cm^{-1})$	(95.600±6.200)
c	$(mol.L^{-1})\times10^{-6}$	(1.1±0.2)
Nanoparticle concentration - Nc	$(cores.L^{-1})\times10^{17}$	(6.7±0.5)

However, before using Equation 7 to estimate the concentration of nanocrystals, it is necessary to standardize the absorbance (Abs_{cal}) obtained from the UV-vis curves. Thus, if the size distribution of the nanocrystals is broader than that of the samples, the absorbance should be corrected using the average HWHM value from the standard samples (HWHM = 14) to fit the results, as follows (Equation 8):

$$Abs_{cal} = Abs\left(\frac{HWHM}{14}\right) \quad (8)$$

The optical properties and concentration parameters calculated from the synthesized nanoparticles are summarized in Table 1.

It was observed that the synthesized CdSe colloidal suspensions were very stable, with a minimum calculated band gap of E_{QD} = 2.20 ± 0.05 eV, which is significantly higher than the CdSe bulk value of 1.74 eV (E_{bulk}). Thus, the estimated blue-shift of approximately 0.46 eV (i.e.,

ΔE = 2.20 - 1.74 eV) proves that CdSe quantum dots were effectively synthesized.

The shell growth was also evidenced by UV-vis spectroscopy results. The shell growth was achieved using the layer-by-layer (LBL) method, through the successive ion layer adsorption and reaction (SILAR) process. Essentially, the PVA-COOH behaves as a ligand for the stabilization of the core (CdSe), but it allows the diffusion of ions (S^{2-} and Cd^{2+}) through the polymer capping layer, leading to the growth of the CdS shell onto the CdSe core. The growth is limited by the depletion of ions in the solution as the shell layer is built. The optical response of CdSe/CdS core-shell type I quantum dots is shown in Figure 2 relative to that of the CdSe core used as "seeds". Due to the growth of the CdS shell, the absorption spectrum roughly maintained its overall shape but shifted to higher wavelengths (lower energies, or a red-shift). A shift of approximately 7 nm (3 meV) accompanied the first S^{2-} stock solution injection (Figure 2b), followed by a shift of 6 nm (2 meV) after the addition of Cd^{2+} and S^{2-} precursors for the second monolayer growth (Figure 2c), leading to a total absorption shift of approximately 13 nm (5 meV) for two monolayers of coverage. As previously reported, this is attributed to the partial leakage of the CdSe exciton through the CdS coating material. The CdS shell affects the electronic state in the CdSe core, as the electrons from the core can easily extend to the CdS shell while the holes remain inside the cores because of their large effective mass. According to Liu et al.[17], the separation of the electron and hole lowers the confinement energy of the exciton, leading to the red-shift observed in the absorption spectra for CdSe/CdS core-shell nanostructures. For that reason, the CdSe/CdS core-shell structure would present different optical behavior than analogous binary alloyed $CdS_xSe_{(1-x)}$ systems[18].

The fluorescence spectra of the core and core-shell structures are shown in Figure 3 ($\lambda_{excitation}$ = 442 nm, with intensities normalized). Three major features of these spectra are most relevant: (i) all spectra consist of a single band associated with the band edge recombination; (ii) no red bands of luminescence, related to intrinsic defects or trap emissions, were observed; and (iii) the thicker the CdS shell covering the CdSe core, the more the fluorescence maximum is shifted to higher wavelengths (red-shift, 17 nm, or lower energies, 6 meV).

The room-temperature PL efficiency was evaluated (Figure 4) and found to increase by approximately 60% when transitioning from the CdSe quantum dot core to CdSe/CdS nanoparticles with one monolayer. This effect was expected, as the general strategy to enhance luminescence involves passivating the surface of nanocrystals by depositing a shell of a wider band-gap semiconductor material (type I core-shell nanocrystals), such as CdS overcoating the CdSe core[19]. The shell physically separates the surface of the optically active core from its surrounding medium, reducing the sensitivity of the optical properties to changes in the local environment at interfaces and the number of dangling bonds that can act as trap states for the photo-generated charge carriers[14,20]. However, at higher coverage, after the growth of the second layer (thicker shell), the efficiency decreased with a resulting reduction of the PL intensity, as already

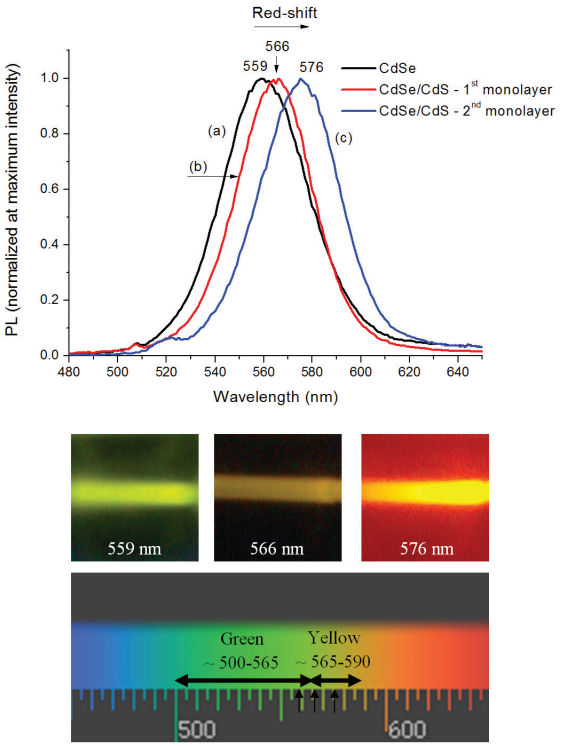

Figure 3. Fluorescence spectra and images of CdSe core (a), CdSe/CdS – 1st monolayer (b) and CdSe/CdS – 2nd monolayer (c) in aqueous colloidal solution excited by laser source at $\lambda_{excitation}$ = 442 nm (normalized intensities).

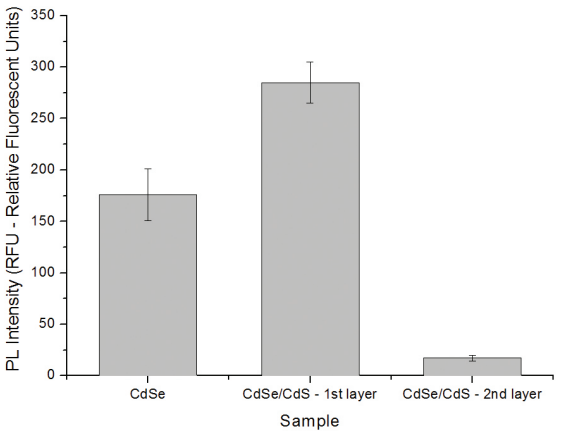

Figure 4. Fluorescence intensity obtained for CdSe core and CdSe/CdS core-shell structures with an excitation wavelength of 365 nm (UV).

reported in the literature[17,21]. This finding was attributed to the generation of misfit dislocations when the thickness of the shell exceeds a critical value and the presence of nonradiative transitions, either at the interface or within the shell, that become the predominant relaxation process.

TEM was used to estimate the nanoparticle size and the size distribution associated with the possibility of evaluating the formation of CdS shell layers onto CdSe core, referred to

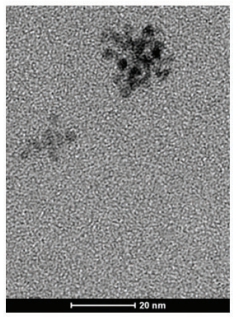

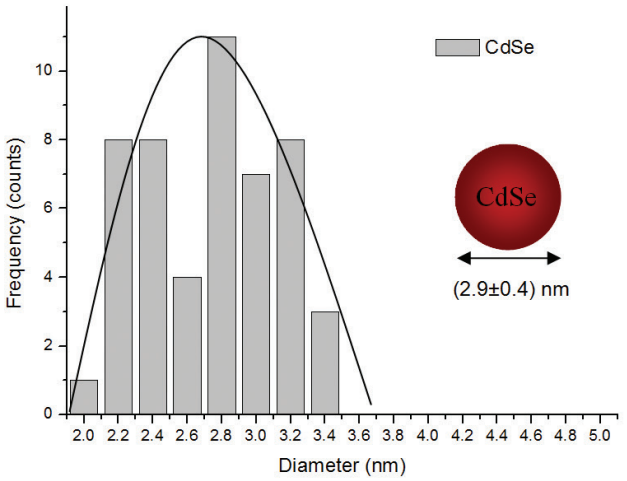

(a)

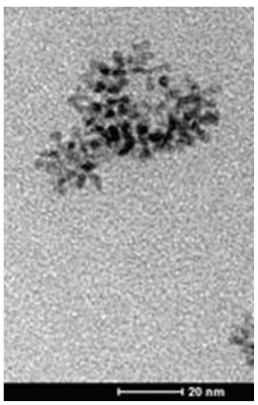

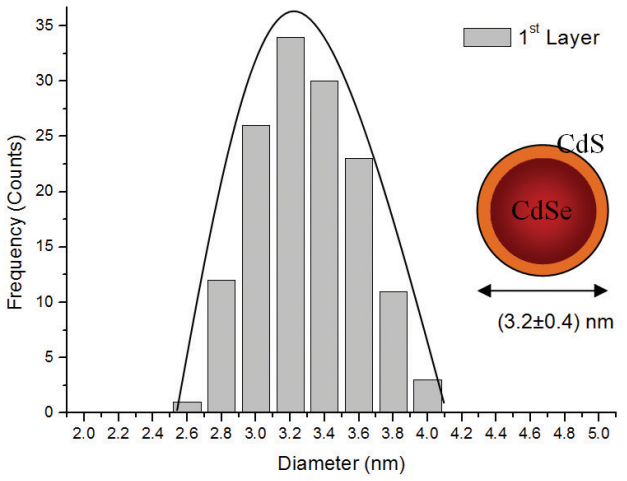

(b)

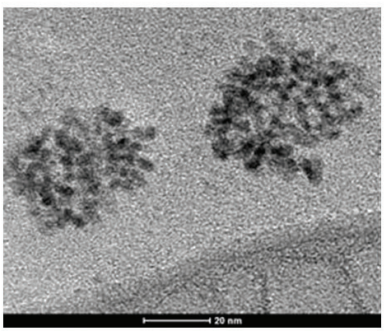

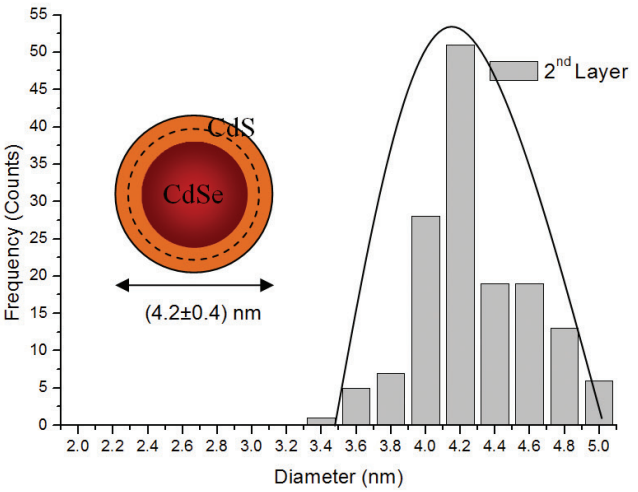

(c)

Figure 5. Histogram of the size distributions based on TEM analysis: CdSe core (a), CdSe/CdS – 1st monolayer (b), and CdSe/CdS – 2nd monolayer (c).

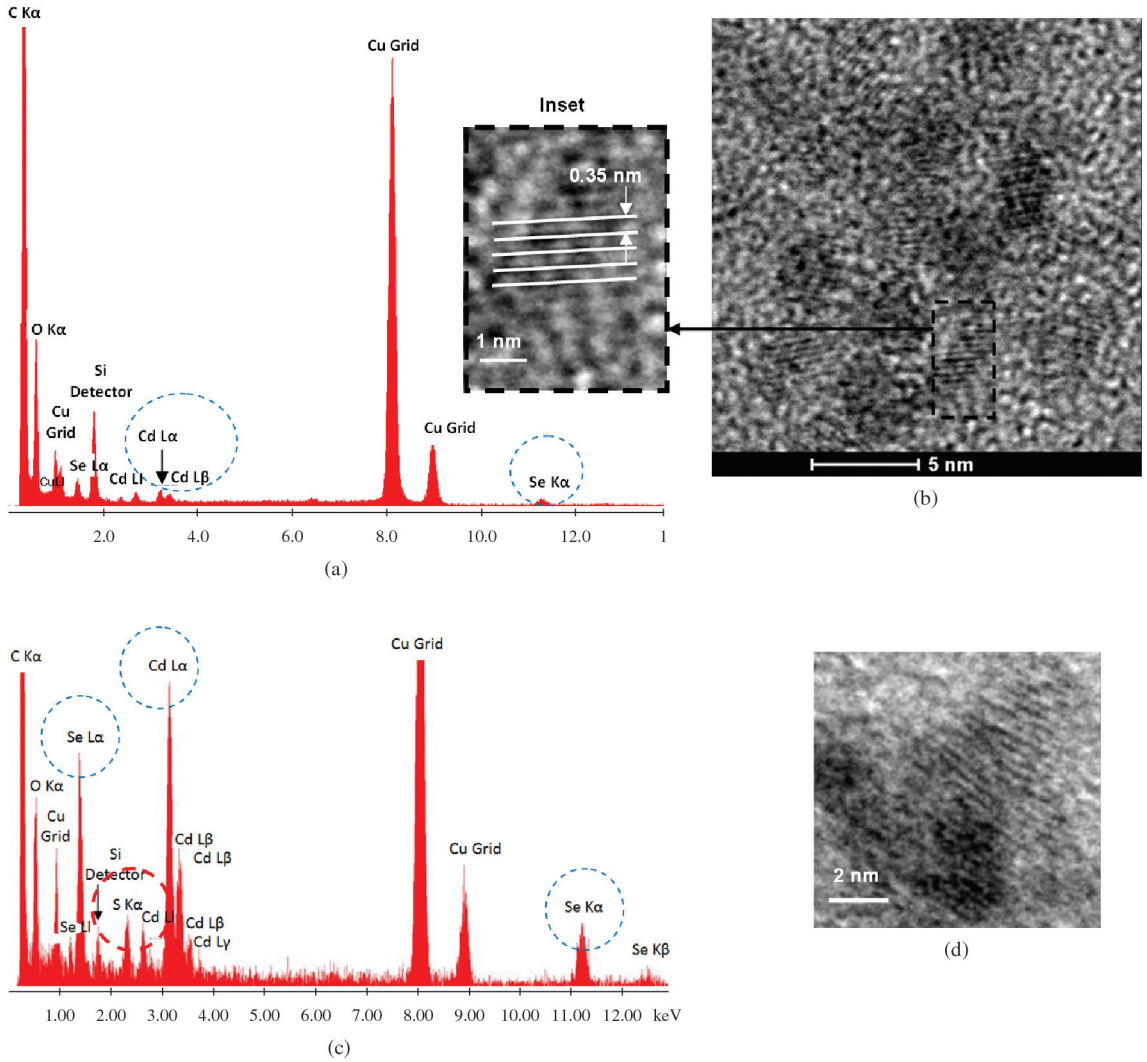

Figure 6. EDS spectra of the CdSe core (a) and CdSe/CdS core-shell-1st monolayer (c). TEM image of the CdSe core (b) and CdSe/CdS core-shell-1st monolayer (d). Inset: lattice arrangements by electron diffraction with detailed nanocrystal plane spacing.

as C-S nanostructures. Figure 5 shows typical TEM images and histograms for the size distributions. CdSe nanocrystals presented a calculated average size of 2.9±0.4 nm, which is comparable to the dimension determined using fitted experimental curves (Table 1). For the core-shell nanostructures, the observed increase in diameter was compatible with the range expected by considering the thickness of each monolayer of the CdS shell, as follows:

- 1st monolayer: Theoretical = 2.9 nm diameter (CdSe core) + 1 monolayer of CdS (0.35 nm × 2) = 3.6 nm; measured result = 3.2±0.4 nm;
- 2nd monolayer: Theoretical = 2.9 nm diameter (CdSe core) + 2 monolayers of CdS (2 × 0.35 nm × 2) = 4.3 nm; measured result = 4.2±0.4 nm.

Representative images of the CdSe core and CdSe/CdS core-shell structure with one monolayer are presented in Figure 6, as well as the corresponding EDS spectra. In a broad sense, most CdSe nanocrystals (Figure 6b) were spherically shaped with resolved lattice fringes with a measured lattice spacing well-matched to the values reported in the literature for CdSe QDs with wurtzite-like crystal structures[22]. For the sample with one monolayer (Figure 6d), these lattice fringes are continuous throughout the entire nanoparticle, evidencing epitaxial growth. Indeed, the main indication of shell growth was the change in the nanocrystal diameter. EDS spectra were used for the chemical analysis of the core nanocrystals, with Cd and Se being the major elements (Figure 6a), excluding the copper, oxygen and carbon peaks related to the TEM grid and PVA polymer stabilizer. The CdSe/CdS core-shell structures presented Cd, Se and S chemical elements (Figure 6c). These TEM/EDS results also support the finding that CdSe QDs and CdSe/CdS core-shell structures were properly stabilized by the PVA-COOH capping polymer.

4. Conclusions

In this research, CdSe/CdS core-shell quantum dots were produced using a “green” route based on aqueous

colloidal chemistry at room temperature. The optical properties of the nanostructured systems were extensively characterized by UV-vis absorption spectroscopy and PL. The morphological and structural aspects were assessed by TEM-EDS analyses associated with electron diffraction patterns. The results have evidenced that CdSe/CdS core-shell structures were formed with enhanced fluorescent behavior relative to the CdSe core. These findings are relevant for the potential applications of these quantum dot fluorophores in biomedical fields, including as biomarkers, in *in vitro* and *in vivo* imaging, and in bio-labeling using an entirely water-based synthesis process.

Acknowledgments

The authors acknowledge financial support from CAPES, FAPEMIG, and CNPq. Additionally, the authors thank the Microscopy Center/UFMG staff for the TEM analysis and Prof. J. González/UFMG for the photoluminescence experiments.

References

1. Brus LE. Electron-electron and electron-hole interactions in small semiconductor crystallites: the size dependence of the lowest excited electronic state. *Journal of Chemical Physics*. 1984; 80:4403-4409. http://dx.doi.org/10.1063/1.447218
2. Mansur HS. Quantum dots and nanocomposites. *Wiley Interdisciplinary Reviews Nanomedicine and Nanobiotechnology*. 2010; 2:113-129. PMid:20104596. http://dx.doi.org/10.1002/wnan.78
3. Park J, Lee KH, Galloway JF and Searson PC. Synthesis of cadmium selenide quantum dots form a non-coordinating solvent: Growth kinetics and particle size distribution. *Journal of Physical Chemistry.* 2008; 112:17849-17854. http://dx.doi.org/10.1021/jp803746b
4. Yordanov GG, Yoshimura H and Dushkin CC. Fine control of the growth and optical properties of CdSe quantum dots by varying the amount of stearic acid in a liquid paraffin matrix. *Colloid Surface A.* 2008; 322:177-182. http://dx.doi.org/10.1016/j.colsurfa.2008.03.002
5. Yu WW, Wang YA and Peng X. Formation and stability of size-, shape-, and structure-controlled CdTe nanocrystals: Ligand effects on monomers and nanocrystals. *Chemistry of Materials.* 2003; 1:4300-4308. http://dx.doi.org/10.1021/cm034729t
6. Mansur HS and Mansur AAP. CdSe Quantum Dots stabilized by carboxylic-functionalized PVA: synthesis and UV-Vis spectroscopy characterization. *Materials Chemistry and Physics.* 2011; 125:709-717. http://dx.doi.org/10.1016/j.matchemphys.2010.09.068
7. Mansur HS, Mansur AAP and González JC. Synthesis and characterization of CdS quantum dots with carboxylic-functionalized poly (vinyl alcohol) for bioconjugation. *Polymer.* 2011; 52:1045-1054. http://dx.doi.org/10.1016/j.polymer.2011.01.004
8. Mansur HS, Mansur AAP and González JC. Biomolecule-quantum dot systems for bioconjugation applications. *Colloid Surface B.* 2011; 84:360-368. PMid:21353498. http://dx.doi.org/10.1016/j.colsurfb.2011.01.027
9. Mansur A, Mansur H and González J. Enzyme-polymers conjugated to quantum-dots for sensing applications. *Sensors*. 2011; 11:9951-9972. PMid:22163736 PMCid:PMC3231291. http://dx.doi.org/10.3390/s111009951
10. Mansur HS and Mansur AAP. Fluorescent Nanohybrids: Quantum-dots Coupled to Polymer-Recombinant Protein Conjugates for the Recognition of Biological Hazards. *Journal of Materials Chemistry.* 2012; 22:9006-9018. http://dx.doi.org/10.1039/c2jm31168b
11. Mansur HS, Mansur AAP, Curti E and De Almeida MV. Bioconjugation of Quantum-dots with Chemically Modified Chitosan. *Carbohydrate Polymers.* 2012; 90:189-196. http://dx.doi.org/10.1016/j.carbpol.2012.05.022
12. Peppas NA and Simmons REP. Mechanistic analysis of protein delivery from porous poly(vinyl alcohol) systems. *Journal of Drug Delivery Science and Technology.* 2004; 14:285-289.
13. Mansur AAP, Ramanery FP and Mansur HS. Water-soluble quantum dot/carboxylic-poly (vinyl alcohol) conjugates: Insights into the roles of nanointerfaces and defects toward enhancing photoluminescence behavior. *Materials Chemistry and Physics.* 2013; 141:223-233. http://dx.doi.org/10.1016/j.matchemphys.2013.05.004
14. Reiss P, Protière M and Liang L. Core/Shell semiconductor nanocrystals. *Small.* 2009; 5:154-168. PMid:19153991. http://dx.doi.org/10.1002/smll.200800841
15. Yu WW, Qu L, Guo W and Peng X. Experimental determination of the extinction coefficient of CdTe, CdSe, and CdS nanocrystals. *Chemistry of Materials.* 2003; 15:2854-2860. http://dx.doi.org/10.1021/cm034081k
16. Dai Q, Li D, Jiang S, Chen H, Wang Y, Kan S et al. Synthesis of monodisperse CdSe nanocrystals directly to air: monomer reactivity tuned by the selenium ligand. *Journal of Crystal Growth.* 2006; 292:14-18. http://dx.doi.org/10.1016/j.jcrysgro.2006.04.097
17. Liu S-M, Guo H-Q, Zhang Z-H, Li R, Chen W and Wang Z-G. Characterization of CdSe and CdSe/CdS core/shell nanoclusters synthesized in aqueous solution. *Physica E.* 2000; 8:174-178. http://dx.doi.org/10.1016/S1386-9477(99)00260-X
18. Mansur HS, Grieser F, Urquhart RS and Furlong DN, photoelectrochemical behaviour of Q-state $CdS_xSe_{(1-x)}$ particles in arachidic acid Langmuir-Blodgett films. *Journal of the Chemical Society, Faraday Transactions.* 1995;91:3399-3404. http://dx.doi.org/10.1039/ft9959103399
19. Sarma DD, Nag A, Santra PK, Kumar A, Sapra S and Mahadevan P. Origin of the enhanced photoluminescence from semiconductor CdSeS nanocrystals. *Journal of Physical Chemistry. Letters.* 2010; 1:2149-2153.
20. Li Y, Zhong H, Li R, Zhou Y, Yang C and Li Y. High-yield fabrication and electrochemical characterization of tetrapodal CdSe, CdTe, and $CdSe_xTe_{1-x}$ nanocrystals. *Advanced Functional Materials.* 2006; 16:1705-1716. http://dx.doi.org/10.1002/adfm.200500678
21. Dabbousi BO, Rodriguez-Viejo J, Mikulec FV, Heine JR, Mattoussi H, Ober R et al. (CdSe)ZnS core-shell quantum dots: synthesis and characterization of a size series of highly luminescent nanocrystallites. *Journal of Physical Chemistry. B.* 1997; 101:9463-9475. http://dx.doi.org/10.1021/jp971091y
22. Zajicek H, Juza P, Abramof E, Pankratov O, Sitter H, Helm M et al. Photoluminescence from ultrathin ZnSe/CdSe quantum wells. *Applied Physics Letters.* 1993; 62:717-719. http://dx.doi.org/10.1063/1.109615